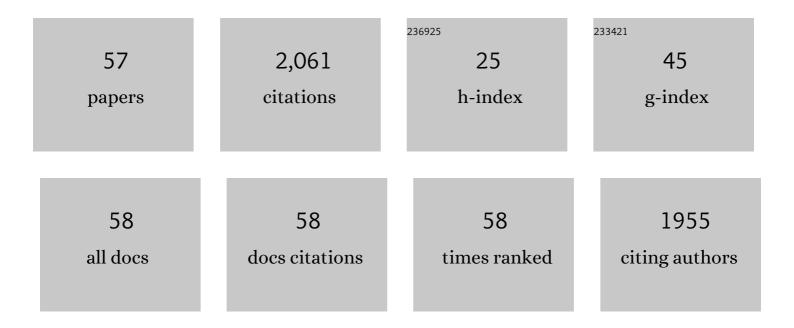
Seok-Woo Lee

List of Publications by Year in descending order

Source: https://exaly.com/author-pdf/838606/publications.pdf Version: 2024-02-01



#	Article	IF	CITATIONS
1	Exercise-induced piezoelectric stimulation for cartilage regeneration in rabbits. Science Translational Medicine, 2022, 14, eabi7282.	12.4	88
2	Heterogeneous Distribution of Mechanical Properties of Single-Particle Cold Spray Impacts. Journal of Thermal Spray Technology, 2022, 31, 498-507.	3.1	3
3	Uniaxial compression of [001]-oriented CaFe2As2 single crystals:the effects of microstructure and temperature on superelasticity Part I: Experimental observations. Acta Materialia, 2021, 203, 116464.	7.9	4
4	Uniaxial compression of [001]-oriented CaFe2As2 single crystals: the effect of microstructure and temperature on superelasticity Part II: Modeling. Acta Materialia, 2021, 203, 116462.	7.9	1
5	Pseudoelasticity of SrNi ₂ P ₂ Micropillar via Double Lattice Collapse and Expansion. Nano Letters, 2021, 21, 7913-7920.	9.1	2
6	Low-temperature failure mechanism of [001] niobium micropillars under uniaxial tension. Journal of Materials Research, 2021, 36, 1-12.	2.6	0
7	Mesoscale modeling of jet initiation behavior and microstructural evolution during cold spray single particle impact. Acta Materialia, 2020, 182, 197-206.	7.9	48
8	Surface states of gas-atomized Al 6061 powders – Effects of heat treatment. Applied Surface Science, 2020, 534, 147643.	6.1	14
9	Ultrahigh elastically compressible and strain-engineerable intermetallic compounds under uniaxial mechanical loading. APL Materials, 2019, 7, .	5.1	8
10	The effect of defects on strength of gold microparticles. Scripta Materialia, 2019, 171, 83-86.	5.2	14
11	Mechanical properties of supersonic-impacted Al6061 powder particles. Scripta Materialia, 2019, 171, 52-56.	5.2	11
12	Effects of temperature on surface-controlled dislocation multiplication in body-centered-cubic metal nanowires. Computational Materials Science, 2019, 168, 172-179.	3.0	4
13	Shear localization and size-dependent strength of YCd6 quasicrystal approximant at the micrometer length scale. Journal of Materials Science, 2018, 53, 6980-6990.	3.7	3
14	Defect structures in solution-grown single crystals of the intermetallic compound Ag3Sn. Journal of Materials Science, 2018, 53, 5317-5328.	3.7	6
15	Modeling pseudo-elastic behavior in small-scale ThCr2Si2-type crystals. Computational Materials Science, 2018, 150, 86-95.	3.0	4
16	Microstructure and Micromechanical Response in Gas-Atomized Al 6061 Alloy Powder and Cold-Sprayed Splats. Journal of Thermal Spray Technology, 2018, 27, 1563-1578.	3.1	29
17	Effects of point defects on the mechanical response of LaRu2P2. Acta Materialia, 2018, 160, 224-234.	7.9	7
18	Insights into the plasticity of Ag3Sn from density functional theory. International Journal of Plasticity, 2018, 110, 57-73.	8.8	6

SEOK-WOO LEE

#	Article	IF	CITATIONS
19	Unraveling the Mesoscale Evolution of Microstructure during Supersonic Impact of Aluminum Powder Particles. Scientific Reports, 2018, 8, 10075.	3.3	31
20	A Nanoindentation Study of the Plastic Deformation and Fracture Mechanisms in Single-Crystalline CaFe2As2. Jom, 2018, 70, 1074-1080.	1.9	4
21	Strong, ductile, and thermally stable Cu-based metal-intermetallic nanostructured composites. Scientific Reports, 2017, 7, 40409.	3.3	6
22	Superelasticity and cryogenic linear shape memory effects of CaFe2As2. Nature Communications, 2017, 8, 1083.	12.8	22
23	Ultrahigh Elastic Strain Energy Storage in Metal-Oxide-Infiltrated Patterned Hybrid Polymer Nanocomposites. Nano Letters, 2017, 17, 7416-7423.	9.1	38
24	Superelastic and micaceous deformation in the intermetallic compound CaFe2As2. Scripta Materialia, 2017, 141, 10-14.	5.2	8
25	Characterization of Dislocations in Single-Crystalline Ag3Sn Intermetallic Alloys. Microscopy and Microanalysis, 2017, 23, 760-761.	0.4	0
26	Observation of asymmetry in domain wall velocity under transverse magnetic field. APL Materials, 2016, 4, 032504.	5.1	11
27	Cross-Split of Dislocations: An Athermal and Rapid Plasticity Mechanism. Scientific Reports, 2016, 6, 25966.	3.3	19
28	Size Effect Suppresses Brittle Failure in Hollow Cu ₆₀ Zr ₄₀ Metallic Glass Nanolattices Deformed at Cryogenic Temperatures. Nano Letters, 2015, 15, 5673-5681.	9.1	77
29	Cold-temperature deformation of nano-sized tungsten and niobium as revealed by in-situ nano-mechanical experiments. Science China Technological Sciences, 2014, 57, 652-662.	4.0	39
30	Cryogenic nanoindentation size effect in [0 0 1]-oriented face-centered cubic and body-centered cubic single crystals. Applied Physics Letters, 2013, 103, .	3.3	26
31	Modeling dislocation nucleation strengths in pristine metallic nanowires under experimental conditions. Acta Materialia, 2013, 61, 2244-2259.	7.9	51
32	Emergence of enhanced strengths and Bauschinger effect in conformally passivated copper nanopillars as revealed by dislocation dynamics. Acta Materialia, 2013, 61, 1872-1885.	7.9	41
33	Emergence of film-thickness- and grain-size-dependent elastic properties in nanocrystalline thin films. Scripta Materialia, 2013, 68, 261-264.	5.2	14
34	Size dependence of the yield strength of fcc and bcc metallic micropillars with diameters of a few micrometers. Philosophical Magazine, 2012, 92, 1238-1260.	1.6	114
35	Higher compressive strengths and the Bauschinger effect in conformally passivated copper nanopillars. Acta Materialia, 2012, 60, 3444-3455.	7.9	68
36	Superplastic Deformation of Defect-Free Au Nanowires via Coherent Twin Propagation. Nano Letters, 2011, 11, 3499-3502.	9.1	189

SEOK-WOO LEE

#	Article	IF	CITATIONS
37	Effects of focused-ion-beam irradiation and prestraining on the mechanical properties of FCC Au microparticles on a sapphire substrate. Journal of Materials Research, 2011, 26, 1653-1661.	2.6	29
38	Size effect in compression of single-crystal gold microparticles. Acta Materialia, 2011, 59, 5202-5215.	7.9	136
39	Dislocation junctions and jogs in a free-standing FCC thin film. Modelling and Simulation in Materials Science and Engineering, 2011, 19, 025002.	2.0	16
40	Micro-pillar plasticity controlled by dislocation nucleation at surfaces. Philosophical Magazine, 2011, 91, 1084-1096.	1.6	63
41	Compression testing of metallic glass at small length scales: Effects on deformation mode and stability. Acta Materialia, 2010, 58, 5789-5796.	7.9	97
42	Geometrical analysis of 3D dislocation dynamics simulations of FCC micro-pillar plasticity. Materials Science & Engineering A: Structural Materials: Properties, Microstructure and Processing, 2010, 527, 1903-1910.	5.6	29
43	Modelling dislocations in a free-standing thin film. Modelling and Simulation in Materials Science and Engineering, 2009, 17, 075007.	2.0	51
44	Uniaxial compression of fcc Au nanopillars on an MgO substrate: The effects of prestraining and annealing. Acta Materialia, 2009, 57, 4404-4415.	7.9	162
45	Dislocation dynamics simulations in a cylinder. IOP Conference Series: Materials Science and Engineering, 2009, 3, 012007.	0.6	5
46	Plasticity criterion for bulk amorphous alloys. Materials Science & Engineering A: Structural Materials: Properties, Microstructure and Processing, 2008, 477, 344-349.	5.6	0
47	Design of a bulk amorphous alloy containing Cu–Zr with simultaneous improvement in glass-forming ability and plasticity. Journal of Materials Research, 2007, 22, 486-492.	2.6	18
48	Self-Aligned Nanolenses with Multilayered Ge/SiO2 Core/Shell Structures on Si (001). Advanced Materials, 2007, 19, 222-226.	21.0	6
49	A parameter governing the plasticity of Cu–Zr containing bulk metallic glasses. Materials Science & Engineering A: Structural Materials: Properties, Microstructure and Processing, 2007, 449-451, 172-175.	5.6	8
50	A high strength Cu-based alloy containing superlattice structures. Scripta Materialia, 2007, 56, 457-460.	5.2	12
51	A Cu-based amorphous alloy with a simultaneous improvement in its glass forming ability and plasticity. Metals and Materials International, 2007, 13, 21-24.	3.4	31
52	Crystallization-induced plasticity of Cu–Zr containing bulk amorphous alloys. Acta Materialia, 2006, 54, 349-355.	7.9	252
53	Mechanism of the deformation-induced nanocrystallization in a Cu-based bulk amorphous alloy under uniaxial compression. Scripta Materialia, 2006, 54, 1439-1444.	5.2	66
54	Pyramid-Shaped Si/Ge Superlattice Quantum Dots with Enhanced Photoluminescence Properties. Advanced Materials, 2006, 18, 367-370.	21.0	8

#	Article	IF	CITATIONS
55	Ferromagnetic formation of two phases due to MnP and InMn3 from InMnP:Zn implanted with Mn (10at.%). Applied Physics Letters, 2006, 88, 232511.	3.3	9
56	Premium 7075 Aluminium Alloys Produced by Reciprocating Extrusion. Advanced Engineering Materials, 2004, 6, 936-943.	3.5	28
57	An Mg-Al-Zn Alloy with Verry High Specific Strength and Superior High-strain-rate Superplasticity Processed by Reciprocating Extrusion. Advanced Engineering Materials, 2004, 6, 948-952.	3.5	25